Paper
Int'l J. of Aeronautical & Space Sci. 17(1), 132–138 (2016)
DOI: http://dx.doi.org/10.5139/IJASS.2016.17.1.132

IJASS
International Journal of Aeronautical and Space Sciences

Aerodynamic Design of the Solar-Powered High Altitude Long Endurance (HALE) Unmanned Aerial Vehicle (UAV)

Seung-Jae Hwang*, Sang-Gon Kim, Cheol-Won Kim** and Yung-Gyo Lee****

Aerodynamic Division, Korea Aerospace Research Institute, Daejeon 34133, Republic of Korea

Abstract

Korea Aerospace Research Institute (KARI) is developing an electric-driven HALE UAV in order to secure system and operational technologies since 2010. Based on the flight tests and design experiences of the previously developed electric-driven UAVs, KARI has designed EAV-3, a solar-powered HALE UAV. EAV-3 weighs 53kg, the structure weight is 22kg, and features a flexible wing of 19.5m in span with the aspect ratio of 17.4. Designing the main wing and empennage of the EAV-3 the amount of the bending due to the flexible wing, 404mm at 1-G flight condition based on T-800 composite material, and side wind effects due to low cruise speed, V_{cr} = 6m/sec, are carefully considered. Also, unlike the general aircraft there is no center of gravity shift during the flight because of the EAV-3 is the solar-electric driven UAV. Thus, static margin cuts down to 28.4% and center of gravity moves back to 31% of the Mean Aerodynamic Chord (MAC) comparing with the previously designed the EAV-2 and EAV-2H/2H+ to upgrade the flight performance of the EAV-3.

Key words: HALE, UAV, Solar-powered, Flexible wing, Ultra-light weight

Nomenclature

AR = Aspect ratio, ~
b_w = Wing span, m
C_D = Drag coefficient of aircraft, ~
C_{D_i} = Induced drag Coefficient of aircraft, ~
C_L = Lift coefficient of aircraft, ~
C_{l_p} = Airplane rolling moment coefficient with change of roll rate, rad^{-1}
C_{l_r} = Airplane rolling moment coefficient with change of yaw rate, rad^{-1}
C_{l_β} = Airplane rolling moment coefficient with angle of sideslip, rad^{-1}
$C_{l_{\delta r}}$ = Airplane rolling moment coefficient with rudder deflection angle, rad^{-1}
C_m = Pitching moment coefficient of aircraft, ~
C_{m_0} = Pitching moment coefficient of aircraft for zero angle of attack, ~
C_{m_α} = Pitching moment coefficient of aircraft with angle of attack, rad^{-1}
$C_{m_{\dot{\alpha}}}$ = Pitching moment coefficient of aircraft with change of angle of attack, rad^{-1}
C_{m_q} = Pitching moment coefficient of aircraft with pitch rate, rad^{-1}
$C_{m_{\delta e}}$ = Pitching moment coefficient of aircraft with elevator deflection angle, rad^{-1}
C_{n_p} = Airplane yawing moment coefficient with change of roll rate, rad^{-1}
C_{n_r} = Airplane yawing moment coefficient with change of yaw rate, rad^{-1}
C_{n_β} = Airplane yawing moment coefficient with angle of sideslip, rad^{-1}
$C_{n_{\delta r}}$ = Airplane yawing moment coefficient with rudder deflection angle, rad^{-1}
C_{y_p} = Airplane side force coefficient with change of roll rate, rad^{-1}
C_{y_r} = Airplane side force coefficient with change of yaw rate, rad^{-1}
C_{y_β} = Airplane side force coefficient with angle of sideslip,

* Senior Researcher, Corresponding author: sjhwang@kari.re.kr
** Researcher, ksg5547@kari.re.kr
*** Principal Researcher, cwkim@kari.re.kr

Received: February 6, 2015 Revised: November 15, 2015 Accepted: : January 14, 2016

http://ijass.org pISSN: 2093-274x eISSN: 2093-2480

rad^{-1}

$C_{y_{\delta r}}$ = Airplane side force coefficient with rudder deflection angle, rad^{-1}

C_w = Mean wing chord length, m

D = Drag force, N

e = Oswald's efficiency factor, ~

L = Lift force, N

P = Power, watt

Re = Reynolds number, ~

S_h = Horizontal tail area, m^2

S_v = Vertical tail area, m^2

S_w = Wing area, m^2

T = Thrust force, N

V = Velocity, m/sec

V_1 = Side wind velocity, m/sec

V_{cr} = Cruise speed, m/sec

V_V = Vertical tail volume coefficient, ~

V_h = Horizontal tail volume coefficient, ~

W = Airplane weight, N

$X_{C.G}$ = Location of center of gravity, m

X_{ac_h} = Location of horizontal tail aerodynamic center, m

X_{ac_v} = Location of vertical tail aerodynamic center, m

y^+ = Non-dimensional wall distance, ~

α = Angle of attack, degree

β = Angle of sideslip, degree

ρ = Density of air, kg/m^3

δ_e = Elevator deflection angle, degree

η = Solar cell energy conversion efficiency, ~

SOC = State of charge, %

ROC = Rate of climb, m/sec

1. Introduction

Since Qinetiq's Zephyr 7 (Maximum Takeoff Weight 53kg, a wing span 22.5m) has successfully flown in the stratosphere, maximum Climb Altitude 21.562km, for two weeks, 336 hours July9~23 2010 [1], High Altitude Long Endurance (HALE) Unmanned Aerial Vehicles (UAVs) are globally developing to substitute a low earth orbit satellite. HALE UAVs that are recyclable and convenient to use are targeting to stay in the stratosphere more than 5 years to compete with the satellite. In the recent years Google and Facebook take over Titan Aerospace and Ascenta to develop an electric-driven HALE UAV that can provide an internet service to Africa to create a new market for them. Following the global trends Korea Aerospace Research Institute (KARI) is also developing an electric-driven HALE UAV since 2010. Electrical Aerial Vehicle (EAV)-1 powered by fuel cell and lithium-polymer battery has developed and completed flight tests in 2011 [2, 3]. EAV-2, which is a concept demonstrator of the hybrid power system with a fuel cell, solar cell and battery, has developed and a first flight test has performed on December 2011. EAV-2 has successfully flown 22 hours in 2012 and climbed up to 5km in 2013. EAV-2H, which is a scale downed version of the EAV-3, powered by an amorphous silicon solar cell and lithium-ion battery has developed and a first flight test has performed on October 2012 [4, 5]. EAV-2H has continuously flown 25.7 hours in 2013. Also, modified version of the EAV-2H, EAV-2H+, has successfully climbed up to an altitude 10km in 2014. KARI's developed EAV series are presented in Fig. 1.

In order to secure system and operational technologies and reduce to risk of the failure of developing a full scale solar-powered HALE UAV, the scale-downed version of the EAV-3, EAV-2H/2H+, has developed first and performed flight tests to verify the conceptual design. Based on the design of EAV-2H/2H+, EAV-3 is developed to verify a climb ability up to an altitude 20km and to demonstrate the developed system's stability and operational feasibility in the severe environment of the stratosphere.

2. Solar-Powered HALE UAV

2.1 History of development of HALE UAV in KARI

KARI has developed the EAV-1, a wing span is 2.4m and total take-off weight is 6.8kg, to secure system and operational technologies for the electric aircraft [3]. Based on the CFD analysis and flight tests of the EAV-1, the mid-size low drag electrical long endurance UAV, EAV-2, has developed. The wing span, wing area, total take-off weight and empty weight of the EAV-2 are 6.93m, $2.09m^2$, 18kg and 11kg, respectably. In order to reduce the total drag of the EAV-2, an aspect ratio (AR) is increased from 8.5 to 20 and a low drag fuselage design and raked wingtip are applied. The total drag in the level flight of the EAV-2 are reduced

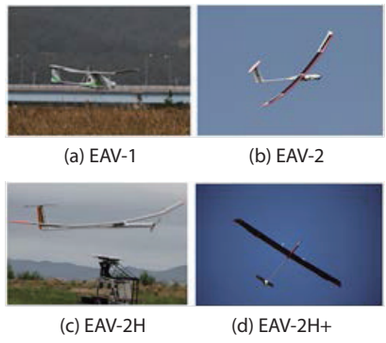

(a) EAV-1 (b) EAV-2

(c) EAV-2H (d) EAV-2H+

Fig. 1. Electric Aerial Vehicle (EAV) Series.

35% comparing with the EAV-1 [4, 5]. After that, the solar-powered scaled HALE UAV, EAV-2H, has developed. The EAV-2H is the scaled-up version of the EAV-2, but an ultra-light weight structural design skill is employed. Even though the wing span (10.83m) and wing area (5.09m^2) of the EAV-2H are increased 56% and 144% comparing to the EAV-2, an empty weight (11kg) of the two aircraft is stayed same and a total weight of the EAV-2H (20kg) is only 2kg heavier than the EAV-2. The structural weight vs. wing loading of the EAV-2, EAV-2H and EAV-3 are plotted in Fig. 2.

Electric motor of the EAV-2H is driven by amorphous solar cells on the main wing and Li-Ion secondary batteries. A SG6043 airfoil that has good aerodynamic characteristics in a low Reynolds number flow (Re ~ 2.0 x 10^5) is selected for the main wing and NACA 0010 and NACA 0012 are selected for the horizontal and vertical tail, respectably. The volume coefficients of the horizontal and vertical tail are 0.57 and 0.028, initially [3, 5]. However, after a couple of test flights of the EAV-2H, the vertical tail volume coefficient is reduce to 0.024 to minimize a side force due to the side wind (V_1) and secure a directional stability at the least, sideslip angle (β) = 25° degree and V_1 = 3.54m/sec. The size of the vertical tail is reduced 15% to cut down 15% of the variation of airplane side force coefficient with sideslip angle, $C_{y\beta}$, and 22% of the variation of airplane side force coefficient with dimensionless rate of change of yaw rate, C_{yr}. Also, the vertical tail to rudder ratio, C_r/C_v, is increased from 30% to 60% to secure the directional stability at the least, the variation of airplane yawing moment coefficient with angle of sideslip ($C_{n\beta}$) = 0.0588rad^{-1} [6, 7].

Based on the design experiences and flight tests of the EAV-1, EAV-2 and EAV-2H/H+, KARI's solar-powered HALE UAV, EAV-3, has designed.

2.2 EAV-3 Design Requirements

The solar-powered HALE UAV, EAV-3, design requirements are as follows:

1. Maximum take-off weight is less than 53kg. (Structure weight is 22kg, weight of Li-Ion batteries is 13kg and weight of on-board system is 18kg).
2. Be able to climb above an altitude 18km (Stratosphere flight, Temperature below -70° C).
3. Minimum energy speed in the level flight is 6m/sec and maximum speed in the level flight is less than 10m/sec in the sea level that allows the EAV-3 is able to operate and pass through a jet stream less than 15m/sec between the altitude 8~12km.

2.3 EAV-3 Power Requirements

Required total power of the EAV-3 is calculated based on a mission profile for the stratosphere flight up to the altitude 18km. A developing purpose of the EAV-3 is obtaining system and operational technologies for the electric driven HALE

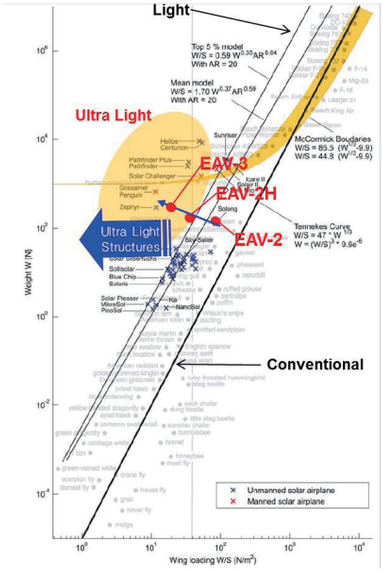

Fig. 2. Structural Weight Comparison of the Electric Aerial Vehicle (EAV) Series.

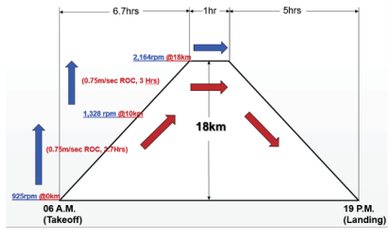

Fig. 3. EAV-3 Mission Profile.

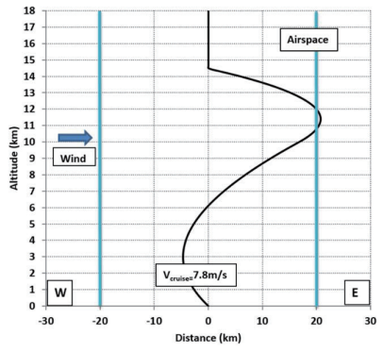

Fig. 4. EAV-3 Calculated Climb Trajectory (Goheung, South Korea in Summer time)

DOI: http://dx.doi.org/10.5139/IJASS.2016.17.1.132

UAV. Thus, the main focus is aimed to the climb ability up to the altitude 18km and operate temperature below -70°C in the challenged stratosphere environment. The EAV-3 mission profile is presented in Fig. 3. Also, the EAV-3 climb trajectory up to the altitude 18km is calculated based on the summer jet stream conditions (less than 15 m/sec) in the Goheung, South Korea. The projected radius of the flight path is 20km. The calculated EAV-3 trajectory is presented in Fig. 4.

Three modules of the mono-crystalline solar cells are attached on the wing of the EAV-3. The solar cell energy conversion efficiency (η) is 23% and the manufactured module efficiency is 21% that generates more than 1.5kWh of energy during the flight. Also, four energy density of 230Wh/kg Li-Ion battery packs are loaded in the EAV-3 that weigh 13kg total and carry 3kWh of energy. The climb time, total power requirement, battery SOC and expected solar power from the solar cells with the rates of climb (ROC) are presented in Fig. 5.

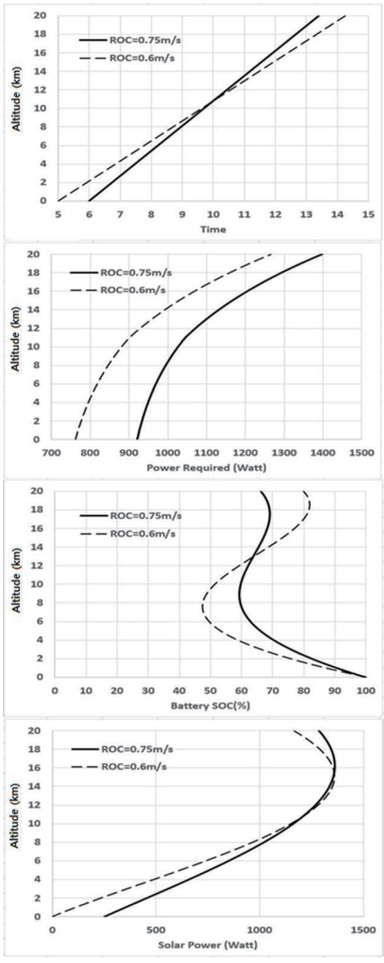

Fig. 5. EAV-3 Climb Time and Power.

2.4 EAV-3 Main Wing Design

The biggest practical limitation of designing the solar-powered HALE UAV is a wing area should be maximized to install the solar panels on the main wing. 490 SunPower mono-crystalline solar cells are used to make three modules. Size of the first and third modules is 2470mm x 950mm and second module is 4100mm x 950mm in width by height. Also, 20% of the leading edge clearance is applied to maintain a laminar flow and delay a transition point over the wing when the modules are mounted on the wing. The solar panel modules mounted on the wing are presented in Fig. 6.

The total available power is 1.5kWh from the solar panels and 3kWh from the 13kg of Li-Ion secondary batteries. The minimum energy cruise speed in the level flight is 6m/sec and a wing root and tip chord is fixed 1300mm and 930mm, respectably. With these limitations the main wing design of the EAV-3 is optimized with following equations:

$$\mathrm{L} = \mathrm{W} = \frac{1}{2} \times \rho \times V^2 \times C_L \times S_w \tag{1}$$

$$\mathrm{D} = \mathrm{T} = \frac{1}{2} \times \rho \times V^2 \times C_D \times S_w \tag{2}$$

$$\mathrm{P} = \mathrm{T} \times \mathrm{V} = \frac{1}{2} \times \rho \times V^3 \times C_D \times S_w \tag{3}$$

Maximum take-off weight (W) = 53kg, C_L = 1.0 and C_D = 400 counts in the level flight conditions are applied to design the EAV-3 as the same conditions have applied to design the previous EAV-2 and EAV-2H [4, 5, 6]. The SG6043 airfoil is consistently maintained for the main wing airfoil of the EAV-3. However, a 4° degree of the dihedral angle that has employed on the main wing of the EAV-2H/H+ has removed to count on the flexibility of the main wing of the EAV-3. The calculated amount of the bending in 1-G flight condition is 404mm based on the T-800 composite material that has applied to manufacture the EAV-3. The amount of bending on the flexible EAV-3 wing has same effects that 4° degree of the dihedral angle applied in the rigid wing. These effects are verified with the Advance Aircraft Analysis Software Package (AAA) [8].

Effects on the induced drag due to change of the aspect ratios are numerically investigated by using the Fluent [9]. The numerical calculations are carried out with S-A turbulence model using patankar and spalding simple algorithm and second order upwind scheme. Dimensionless wall distance (y^+) < 1 is kept and 8~13 million meshes are used. The initial conditions employed for the CFD analysis are V = 6m/sec, Re = 5 x 10^5 and 4° degree of angle of attack (C_L = 1.0). The numerical results are presented in Table 1.

As the aspect ratio increases from 14.8 to 20, the amount of the drag decreases 12.5% (51 counts). It well matches

a general tendency that as the aspect ratio increases, the induced drag of the wing decreases and the aerodynamic performance of the aircraft is enhanced. However, the EAV-3 has the flexible wing and ultra-light weight design concept is employed. As the aspect ratio is increased, the wing span is enlarged and wing root chord is shorten. As a result, the center of gravity of the wing moves toward the wing tip and the amount of the bending is also increased that degrades the aerodynamic performance of the wing. To prevent the adverse effect a stiffness of the wing has to be increased that results the structure weight increment and makes to consume more energy in the flight. Therefore, the aspect ratio of the EAV-3 is selected 17.4 that satisfies the structure weight restriction of the 22kg and maximizes the aerodynamic performance of the EAV-3 at the same time. Also, the raked-wingtip is applied to reduce the induced drag of the wing. The raked-wingtip reduces 3.4% of the drag [10].

The designed EAV-3 wing has the wing span (b) = 19.5m and wing area (S_W) = 21.84m^2 with the raked-wingtip and no dihedral angle. The wing is presented in Fig. 7.

2.5 EAV-3 Empennage Design

The empennage of the EAV-3 has designed based on the EAV-2H empennage design and previous flight tests. In general aircraft design a vertical tail chord to a rudder chord ratio (C_r/C_V) is limited less than 30%, but the ratio is increased up to 60% to make up the large aspect ratio and flexible wing and to cover up vulnerability due to side wind because of the low cruise speed (V = 6 ~ 10m/sec). Also, to minimize a side force due to the side wind two factors are primarily considered. One is a design guideline to secure a directional stability at the least that is the variation of airplane yawing moment coefficient with angle of sideslip, $C_{n\beta}$, is greater than 0.0573rad^{-1} [11, 12]. The other one is a vertical tail volume coefficient (V_V). The vertical tail volume coefficient of the glider or sailplane is typically between 0.02 and 0.07, but recently developed HALE UAVs have the vertical tail volume coefficient less than 0.02. For example, Perseus B has 0.015, Theseus has 0.011 and Condor has 0.011. However, securing the directional stability at the least is considered the first priority to design the vertical tail of the EAV-3. The horizontal tail volume coefficient (V_h) of the EAV-3 is designed same as the glider or sailplane volume coefficient that is between 0.3 and 0.66.

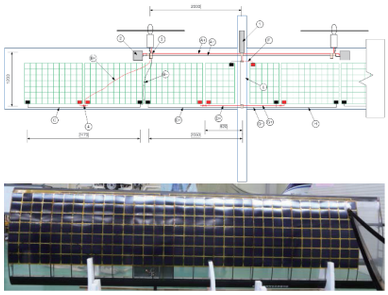

Fig. 6. Solar panels on the wing of EAV-3.

Table 1. Aspect ratio vs. C_D (V=6m/sec, α=4°degree, Re=5×10^5, Wing only)

	EAV-2H	EAV-3	EAV-3	EAV-3
AR	23	20	17.4	14.8
S_W (m^2)	5.09	21.84	21.84	21.84
C_D at C_L=1.0	0.0330	0.0358	0.0379	0.0409
e	0.465	0.526	0.581	0.639
C_{D_i}	0.0298	0.0303	0.0315	0.0336

Vertical tail volume coefficient (V_V):

$$V_V = \frac{S_v \times (X_{ac_v} - X_{C.G})}{S_w \times b_w} \quad (4)$$

Where $V_V \equiv$ Vertical tail area, (X_{acV}-$X_{C.G}$) $\equiv$ Moment arm of the vertical tail, $S_W \equiv$ Wing Area and $b_w \equiv$ Wing span.

Horizontal tail volume coefficient (V_h):

$$V_h = \frac{S_h \times (X_{ac_h} - X_{C.G})}{S_w \times C_w} \quad (5)$$

Where $S_h \equiv$ Horizontal tail area, (X_{acV}-$X_{C.G}$) $\equiv$ Moment arm of the horizontal tail and $C_W \equiv$ Mean wing chord length.

The Designed horizontal tail and vertical tail volume

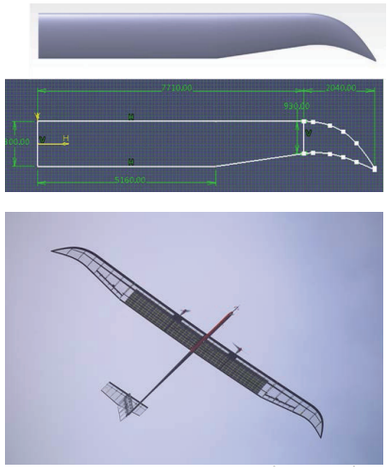

Fig. 7. EAV-3 Planform Design (AR = 17.4).

DOI: http://dx.doi.org/10.5139/IJASS.2016.17.1.132

coefficient of the EAV-3 are 0.55 and 0.0215, respectably. The airfoils of the horizontal and vertical tail are NACA 0010 and NACA 0012 that are consistently kept the same as the EAV-2 and EAV-2H/H+. The variation of airplane yawing moment coefficient with angle of sideslip, $C_{n\beta}$, of the EAV-3 is 0.0574rad^{-1} to secure the directional stability at the least.

2.6 Aerodynamic and Stability

In general an airplane has typically the pitch down moment and redeems it with the horizontal tail in a level flight to secure the longitudinal stability. This notion is also applied to design the EAV-2H and EAV-3. Static margin and center of gravity of the EAV-2H are 56.6% and 25% of the mean aerodynamic chord (MAC), respectably. However, static margin of the EAV-3 is reduced 28.4% and center of gravity of the EAV-3 also moves back 31% of the MAC to reflect the two years of the EAV-2H/2H+ flight test results. As reducing the static margin lift to drag ratio, L/D, is improving that is enhancing the performance of the EAV-3. Also, based on the preliminary design studies with the AAA [8] when the center of gravity of the EAV-3 is located at 25% of the MAC, the all moveable horizontal tail has to deflect to -5° degree to redeem the pitch down moment in the level flight. However, when the center of gravity moves back from 25% to 31% of the MAC, the required horizontal tail deflection is less than -2° degree. Thus, the trim drag due to the horizontal tail deflection can be minimized in the level flight. The trim drag increments due to the horizontal tail deflections are numerically inspected with the Fluent. The generated grids and numerical results are presented in Fig. 8. ~ 10. The sizing and schematic drawing of the EAV-3 are presented in Table 2 and Fig. 11.

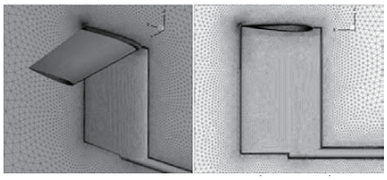

Fig. 8. EAV-3 Empennage (δ_e=-2°).

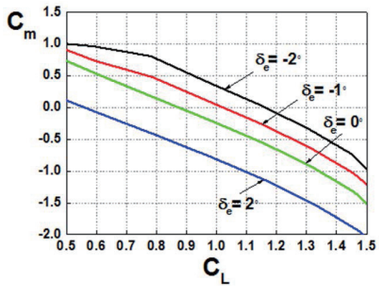

Fig. 9. EAV-3 C_m vs. δ_e.

The EAV-3 sizing and aerodynamic and stability derivatives are preliminarily designed and checked with the AAA. Also, aerodynamic and stability derivatives are numerically verified with the Fluent. The initial flight conditions are V = 6m/sec and altitude = 300m. The longitudinal and directional stabilities are initially judged with the sign (+/-) of the coefficients. As the angle of attack or pitch rate is increasing, the pitching moment of the EAV-3 is becoming more negative. Thus, the

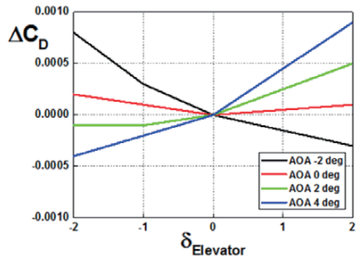

Fig. 10. EAV-3 Trim Drag.

Table 2. Sizing of EAV-2H vs. EAV-3

	EAV-2H	EAV-3
AR	23	**17.4**
Length	5 m	**9 m**
Height	0.944 m	**1.56 m**
Span	10.83 m	**19.5 m**
Wing Area	5.09 m^2	**21.84 m^2**
Horizontal Tail Area	0.40 m^2	**2.27 m^2**
Vertical Tail Area	0.345 m^2	**1.56 m^2**
Fuselage	2.15 m	**3.4 m**
Take-off Weight	20kg	**53kg**

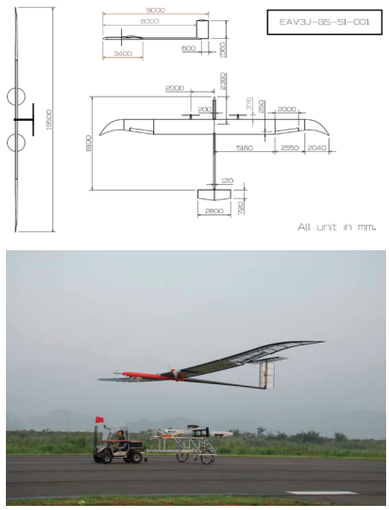

Fig. 11. Schematic Drawing of EAV-3.

Table 3. Comparison of the Aerodynamic and Stability Derivatives

Pitching moment coefficients (AAA)

Symbol	EAV-2H	EAV-3
C_{m_0}	-0.2408	**-0.0745**
C_{m_α}	-2.89 rad^{-1}	**-1.47 rad^{-1}**
C_{m_α}	-4.15 rad^{-1}	**-3.09 rad^{-1}**
C_{m_q}	-39.47 rad^{-1}	**-20.69 rad^{-1}**
$C_{m_{\delta e}}$	-2.53 rad^{-1}	**-1.96 rad^{-1}**
Static Margin	56.6 %	**28.4 %**

Static Stability derivatives (AAA)

Symbol (rad^{-1})	EAV-2H	EAV-3	Stable Criteria
C_{y_β}	-0.168	**-0.199**	**< 0**
C_{y_p}	-0.041	**-0.061**	**< 0**
C_{y_r}	0.113	**0.112**	**> 0**
$C_{y_{\delta r}}$	0.124	**0.165**	**> 0**
C_{l_β}	-0.060	**-0.055**	**< 0**
C_{l_p}	-0.556	**-0.553**	**≪ 0**
C_{l_r}	0.259	**0.351**	**> 0**
$C_{l_{\delta r}}$	0.0054	**0.0031**	**> 0**
C_{n_β}	0.0588	**0.0574**	**> 0**
C_{n_p}	-0.124	**-0.174**	**< 0**
C_{n_r}	-0.065	**-0.067**	**< 0**
$C_{n_{\delta r}}$	-0.041	**-0.052**	**< 0**

longitudinal stabilities of the EAV-3 are properly obtained. As inspecting carefully the signs of the stability coefficients, all of the directional stabilities are met the requirements. The EAV-3 is designed to minimize the side wind effects to secure the directional stabilities at the least, $C_{n\beta}$ = 0.0574rad^{-1}. Also, the amount of bending, 404mm at 1-G flight, due to the flexible wing has the same effect as 4° degree of the dihedral angle. Thus, when the sideslip occurs, the rolling moment occurs to the opposite direction to obtain the static stabilities. All of the calculated static stability coefficients are presented in Table 3.

3. Conclusion

The KARI's Solar-powered HALE UAV, EAV-3, is developed to secure the system and operational technologies for the electric driven HALE UAV. The designed EAV-3 has the aspect ratio 17.4 and maximum take-off weight 53kg. When EAV-3 is designed, the flexible wing, 404mm bending at 1-G, and vulnerability to the side wind due to the low cruise speed, V = 6 ~ 10m/sec, are carefully considered. Also, based on the several years of the flight tests of the electric driven UAVs, EAV-1, EAV-2 and EAV-2H/H+, the static margin is reduced from 56.6% to 28.4% and the center of gravity is moved back from 25% to 31% of the mean aerodynamic chord to improve the performance and reduce the flying power consumption of the EAV-3.

References

[1]"FAI Record ID No. 16052", Federation Aeronautique International. Retrieved 4 December 2012.

[2] Jin, W., Lee, Y., Kim, C., Ahn, S. and Lee, D., "Computational Analysis of Aerodynamic Performance of a Small-Scale Electric Aerial Vehicle", *Proceeding of the 2010 Korean Society for Aeronautical & Space Sciences (KSAS) Fall Conference*, Vol. 1, 2010, pp. 473-476.

[3] Korea Aerospace Research Institute, "System and Operational Technology Research for Electric Airplane (I)", 2011.

[4] Jin, W., Lee, Y., Kim, C. and Ahn, S., "Initial Design and Computational Aerodynamic Analysis of a Medium Electric Aerial Vehicle", *Proceeding of the 2011 Korean Society for Aeronautical & Space Sciences (KSAS) Spring Conference,* Vol. 1, 2011, pp. 850-855.

[5] Korea Aerospace Research Institute, "System and Operational Technology Research for Electric Airplane (II)", 2012.

[6] Korea Aerospace Research Institute, "System and Operational Technology Research for Electric Airplane (III)", 2013.

[7] Hwang, S., Lee, Y., Kim, C. and Ahn, S., "Empennage Design of Solar-Electric Powered High Altitude Long Endurance Unmanned Aerial Vehicle", *J. of the Korean Society for Aeronautical and Space Sciences (KSAS)*, Vol. 41, No. 9, 2013, pp. 708-713.

[8] Advanced Aircraft Analysis Software Package (AAA), Ver. 3.2, DARCorporation, Lawrence, KS, USA.

[9] ANSYS FLUENT Ver. 12 Software Package, Ansys Fluent Inc., Canonsburg, PA, USA.

[10] Jin, W. and Lee, Y., "Drag Reduction Design for a Long-endurance Electric Powered UAV", *International Journal of Aeronautical and Space Sciences*, Vol. 16, No. 2, 2015, pp. 311-324.

[11] Roskam, J., "Airplane Design Part III: Layout Design of Cockpit, Fuselage, Wing and Empennage: Cutways and Inboard Profiles", DARCorp., Lawrence, KS, USA, 2004.

[12] Roskam, J., "Airplane Design Part VII: Determination of Stability, Control and Performance Characteristics: FAR and Military Requirements", DARCorp., Lawrence, KS, USA.

DOI: http://dx.doi.org/10.5139/IJASS.2016.17.1.132